Supporting Information For:

Advanced Oxidation Kinetics and Mechanism of Preservative Propylparaben Degradation in Aqueous Suspension of TiO$_2$ as well as Risk Assessment of Its Degradation Products

Hansun Fang,†, ‖ Yanpeng Gao,†, ‖ Guiying Li,†   Jibin An,†, ‖ Po-Keung Wong,‡ Haiying Fu,§ Side Yao,§ Xiangping Nie, ⊥ and Taicheng An*,†

*Corresponding Author: **Prof. Taicheng An**: Tel +86-20-85291501; E-mail antc99@gig.ac.cn

Numbers of pages: 33

Tables:

Figures:

Experimental Details

Photocatalytic Degradation Experiments. Photocatalytic degradation of PPB was performed in a Pyrex reactor with a 125 W high-pressure mercury lamp as a light source. Prior to illumination, a suspension of 150 mL 100 μM PPB with various contents of photocatalyst (Degussa P25) was stirred in the dark for 30 min to achieve the adsorption-desorption equilibrium. 3.0 mL reaction solutions were sampled at required intervals and filtered through 0.2 μm Millipore membrane for later analysis. The concentration of PPB was measured by Agilent 1200 series high performance liquid chromatography (HPLC) with photodiode array detector set at 255 nm. Separation was achieved on an Agilent C18 column (4.6×250 mm, 5 μm particle diameter) 10 μL filtered sample was injected for analysis. The eluent was a mixture of 70% methanol and 30% ultra-pure water containing 10 mM KH_2PO_4 with 0.8 mL min^{-1} flow-rate.

■ RESULTS AND DISCUSSION

The optimization of photocatalytic degradation of PPB in water

The most widely used Langmuir-Hinshelwood (L-H) model was used to describe the photocatalytic degradation kinetics with the value of pseudo-first-order rate constant as shown in Eq. (1) [1]:

$$\ln\frac{C_t}{C_0} = k_1 t \quad (1)$$

where k_1 is the pseudo-first-order rate constant (min^{-1}), t is the photocatalytic degradation time (min), and C_0 and C_t refer to the concentration of PPB (μM) at the beginning and at the photocatalytic time t, respectively.

Kinetics studies suggested that PPB can be photocatalytic degraded quickly within 120 min in suspension of TiO$_2$. The photocatalytic degradation of PPB can fit the L-H model well within 60 min photocatalytic degradation with little influence of the products under all the experimental conditions. Hence, to understand the adsorptive property on the photocatalytic degradation of PPB, a transformed L-H model was employed to analyze the data obtained at different initial concentrations of PPB as shown in Eq. (2). [2]

$$\frac{1}{r} = \frac{1}{kKC} + \frac{1}{k} \quad (2)$$

where r is initial degradation rate (μM min^{-1}), k is intrinsic reaction rate constant (μM min^{-1}), K is the L-H adsorption constant (μM^{-1}), and C is PPB concentration at adsorption equilibrium (μM).

Figure S4 shown a plot of Eq. (2), and the value of k and K are calculated as 3.01 μM min^{-1} and 0.03 μM^{-1}, respectively. This adsorption constant is close to the values of β-blockers described in our previous paper, [3] indicating that the adsorption performance may also affect

photocatalytic degradation of PPB. To further explore the role of adsorption, the adsorption-desorption equilibrium was also measured within 30 min at various pH conditions based on the assumption that the adsorption performance of PPB onto catalyst could be affected by different pH values.[4, 5] As Figure S5 showed that the adsorption of PPB is more efficient in acid and neutral media (with 2.3%, 5.2% and 5.6% at pH 3.0, 5.0 and 7.0, respectively) than those in alkaline media (with 2.1% and 0% at pH of 9.0 and 11.0, respectively). With pKa value of 8.24,[6] PPB is tend to exist mainly with the neutral form with a small dissociation of PPB which can be adsorbed onto the positive charged catalyst surface below the zero point of TiO_2 (pH value 6.2). On the other hand, with further increase of the pH value above 8.24, PPB was transformed to its anionic form (Figure S6), which is difficult to adsorb onto the negative charged TiO_2, thus the degradation efficiencies was decrease fast with further increase pH value of solution.

UPLC/MS/MS analysis of photocatalytic degradation products

m/z 195. Four products are detected with m/z 195 atomic mass units (amu) with t_R at 2.32, 2.48, 3.29 and 5.41 min, respectively. An increase of 16 in the m/z molecular ion of parent compound (m/z 179) indicates the monohydroxylation onto the aromatic ring or the propyl ester chain of PPB. The products C and D obtain similar fragment patterns as the parent compound as shown in Figure S9 (a-c), which possess the main ions of m/z 92, 93, 136 and 137. The results indicate that these two products are corresponding to the PPB monohydroxylated onto the propyl ester chain. Furthermore, the ratio of m/z 92 against 93 of the compound with product C is 1.47, lower than that of product D with a value of 6.66. The difference suggests that the O-H bond adducted to the alkyl chain of the former is more easily

dehydrogenated as compared with the latter under the same negative ionization condition. Hence, the 1-Hydroxy-propyl, 4-hydroxybenzoate with a weaker O-H bond is believed to be the compound with t_R at 2.32 min, and 2-Hydroxy-propyl, 4-hydroxybenzoate are believed to be the other. Figure S9 (d-g) also showed the fragmentation patterns of the compounds E and I. As can be seen, these two compounds are characterized with the fragment ion m/z 108, which is 16 amu higher than the main fragment ion of PPB with m/z 92, indicating the monohydroxylated adduct onto the aromatic ring. Furthermore, the fragments m/z 152 and 153 are only detected for the compound I, and with the same collision energy (CE=12 V). This compound possess a relative low abundance of m/z 108, indicating that an enhanced interatomic force such as the intramolecular hydrogen bonding may be introduced to this compound through the monohydroxylation process. Hence, the 2-hydroxy-propyl paraben with a carbonyl substituent at the ortho position is supposed to be the structure of compound I, while the other is identified as the 3-hydroxy-propyl paraben.

m/z 211. Three products are detected at m/z 211 with t_R at 1.42, 3.95 and 4.61min, and the fragmentation patterns are given in Figure S9 (h-l). An increase of 16 amu in the m/z molecular ion of m/z 195 indicates that dihydroxylated products are formed during the further photocatalytic oxidation process of PPB. The main fragmentation ions of the compound B are m/z 93 and 137 without m/z 108 and 109, presenting the characteristic fragments of the products hydroxylated at the alkyl chain as mentioned above. Hence, compound B is proposed to be the 1,2-dihydroxy-propyl, 4-hydroxybenzoate, which probably comes from the further oxidation of 1-Hydroxy-propyl, 4-hydroxybenzoate or 2-Hydroxy-propyl, 4-hydroxybenzoate with HO·. The relatively short retention time of this compound also

suggested its high hydrophilicity after hydroxylation onto the alkyl chain. The fragmentation ions m/z 109 and 92 are observed from the compounds G and H. The m/z 109 is proposed to be the fragment ion of dihydroxybenzene, while the m/z 92 is the 17 amu less than m/z 109, indicating the loss of a -OH. Besides the -OH on the aromatic ring, the other 16 amu increase is probably due to the hydroxylation onto the alkyl chain. Hence, further study on fragmentation patterns of the two compound with lower collision energy (CE=10V) is performed as shown in plot Figure S9 (i) and (k). As can be seen, the ratio of m/z 136 against 137 of products G and H are 1.54 and 2.97, respectively, suggesting that the former possess a O-H bond adducted to the alkyl chain which is more easily dehydrogenated. The fragment ion intensity of m/z 193 of product H is stronger than that with product G, and the 18 amu decease is due to the lose of a H_2O, suggesting the former obtains a more stable O-H bond on the alkyl chain that could not be easily ionized. Hence, the 1-hydroxy-propyl, dihydroxybenzoate and 2-hydroxy-propyl, dihydroxybenzoate are proposed as the structures of the products with t_R at 3.95 and 4.61 min, respectively.

m/z 193. One product is detected at m/z 193 with t_R at 3.61 min, a decrease by 2 amu of the monohydroxylated products (m/z 195). The main fragments of this product are m/z 92 and m/z 136 as shown in Figure S9 (m), which are similar with the fragment patterns of products C, D and PPB. The 2 amu loss is probably attribute to the replacement of -OH with carbonyl group (=O) on the alkyl chain. Further more, the fragment ion of m/z 149 indicates that this product is probably the β-ketone compound. Hence, the structure is proposed as 2-ketone-propyl, 4-hydroxybenzoate.

m/z 137. One product is detected at m/z 137 with t_R at 0.97min with its fragmentation pattern in Figure S9 (n). This compound is identified as 4-hydroxybenzoic acid, which is confirmed by the authorized standard on the aspects of the fragmentation patterns as well as the retention time (Figure S11).

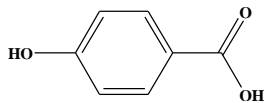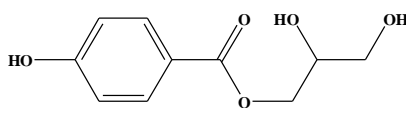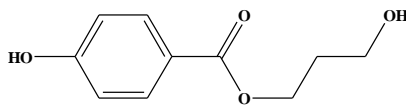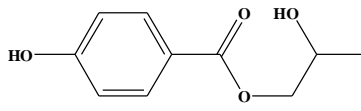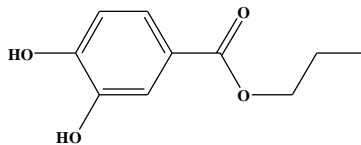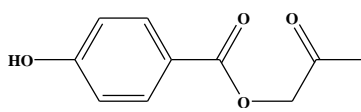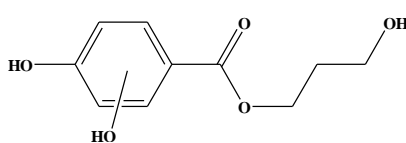**Table S1** Direct photolysis and photocatalytic degradation of PPB influenced by TiO_2 dosage, PPB concentration and pH value.

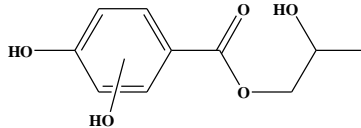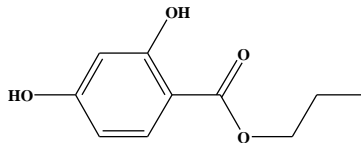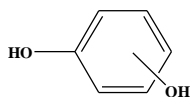| Experimental conditions		k_1 (min^{-1})	R^2	Half life (min)
Direct photolysis	-	0.0002	0.952	3465.7
TiO_2 dosage (g L^{-1})	0.5	0.0187	0.992	37.1
	1.0	0.0237	0.991	29.2
	2.0	0.0272	0.989	25.5
	3.0	0.0293	0.991	23.7
	4.0	0.0301	0.989	22.8
PPB concentration (μM)	20	0.1962	0.966	3.5
	50	0.0640	0.972	10.8
	100	0.0272	0.992	25.5
	200	0.0142	0.996	48.8
pH value	3.0	0.0286	0.995	24.2
	5.0	0.0281	0.999	24.7
	7.0	0.0271	0.993	25.6
	9.0	0.0239	0.994	29.0
	11.0	0.0091	0.999	76.2

Table S2 Experimental conditions, purpose, and the rate constants for photocatalytic degradation of PPB with various scavengers' addition.

Experimental conditions	Purpose	k_1 (min^{-1})
No scavengers	/	0.0272
0.1 M Isopropanol	Quench $HO^{\bullet}$[3]	0.0042
0.1 M Methanol	Quench $HO^{\bullet}$ and h^+[7]	0.0023
0.1 M KI	Quench h^+ and $HO^{\bullet}_{ads}$[8]	0.0080
0.1 mM NaF	Increase $HO^{\bullet}_{bulk}$[9]	0.0514
Dissolved in MeCN	Exclude $HO^{\bullet}$[10, 11]	0.0188
50 μM $K_2Cr_2O_7$	Quench e^-_{aq}[12]	0.0056
0.1 M KI + 0.1 M isopropanol + N_2	Reserve only e^-_{aq}[13]	0.0004
0.1 M KI + 0.1 M isopropanol + O_2	Reserve oxidative species except for $HO^{\bullet}$ and h^+[14]	0.0089
10 μM Fe (II)-EDTA	Quench H_2O_2[13, 15]	0.0195

Table S3 Compounds identified by UPLC/MS/MS (a) and SPE/GC/MS (b) during the photocatalytic degradation of PPB.

	Products	t_R (min)	Molecule weight	Supposed structure	LC_{50} (Daphnid) mg L^{-1}	EC_{50} (Green algae) mg L^{-1}
(A)	4-Hydroxybenzoic acid*	0.97 [a]	138		159.249	776.856
(B)	1, 2-Dihydroxy-propyl,4-hydroxybenzoate	1.42 [a]	212		91.635	493.210
(C)	1-Hydroxy-propyl,4-hydroxybenzoate	2.32 [a]	196		19.345	93.277
(D)	2-Hydroxy-propyl,4-hydroxybenzoate	2.48 [a] 26.31 [b]	196		21.292	103.402
(E)	2-Hydroxypropyl paraben	3.29 [a] 23.88 [b]	196		107.363	1.721
(F)	2-Ketone-propyl,4-hydroxybenzoate	3.61 [a] 16.04 [b]	194		21.389	103.988
(G)	1-Hydroxy-propyl,dihydroxybenzoate	3.95 [a]	212		859.013	2.227

(H)	2-Hydroxy-propyl,dihydroxybenzoate	4.61 [a]	212	978.295	2.261
(I)	3-Hydroxypropyl paraben	5.41 [a] 17.78 [b]	196	11.646	1.332
(J) (K)	Dihydroxybenzene	13.66 [b] 22.91 [b]	110	255.855	1.141

[*]Authentic standards are available

Table S4 The absolute bimolecular reaction rate constants of HO$^{\bullet}$ with propylparaben, ethylparaben and 4-hydrobenzoic acid obtained by both pulse radiolysis and the competitive method.

Name	k_T (M^{-1} s^{-1})	k_A (M^{-1} s^{-1})	k_H (M^{-1} s^{-1})	k_H %
Propylparaben	$7.70\pm0.38\times10^{9}$	$4.65\pm0.23\times10^{9}$	$3.05\pm0.15\times10^{9}$	39.6
Ethylparaben	$7.12\pm0.36\times10^{9}$	$5.36\pm0.27\times10^{9}$	$1.76\pm0.09\times10^{9}$	24.7
4-Hydrobenzoic acid	$6.65\pm0.33\times10^{9}$	$7.07\pm0.35\times10^{9}$	$<0.69\times10^{9}$	<9.8
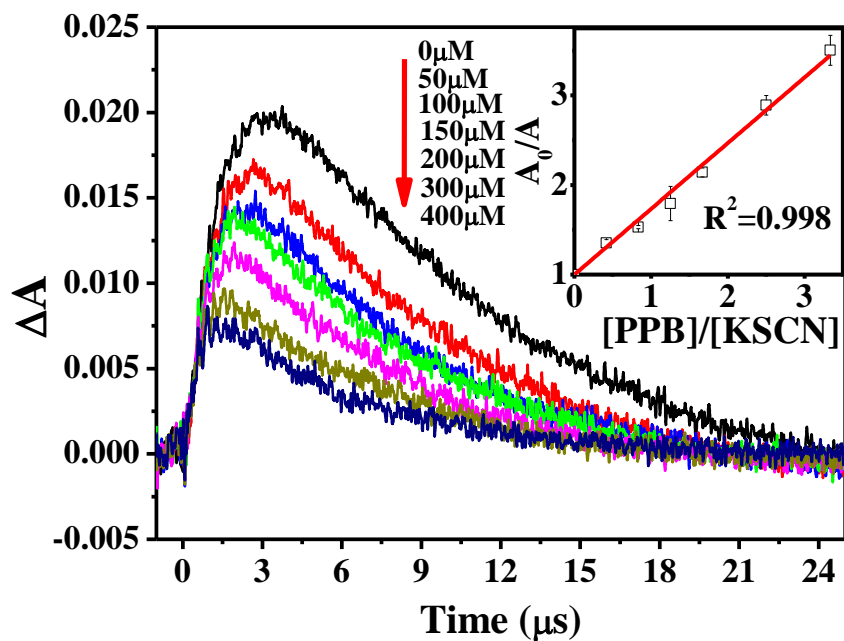
Figure S1 Kinetics observed for N_2O-saturated 120 μM KSCN solutions at 480 nm with different PPB concentrations. Inset represents the competitive plot as a function of the PPB/KSCN relative concentration with a slope of 0.73.
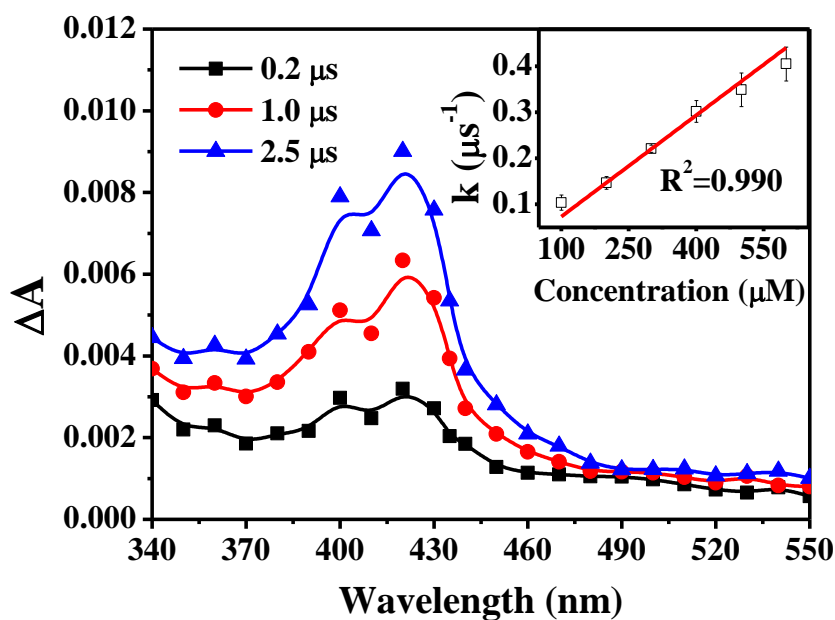
Figure S2 Difference adsorption spectra generated from the reaction of 400 μM PPB with $^{\bullet}N_3$ saturated with N_2O at different time intervals. Inset represents the plot of the pseudo-first-order transient formation rate constants at 420 nm vs. different PPB concentrations in the reaction with $^{\bullet}N_3$.
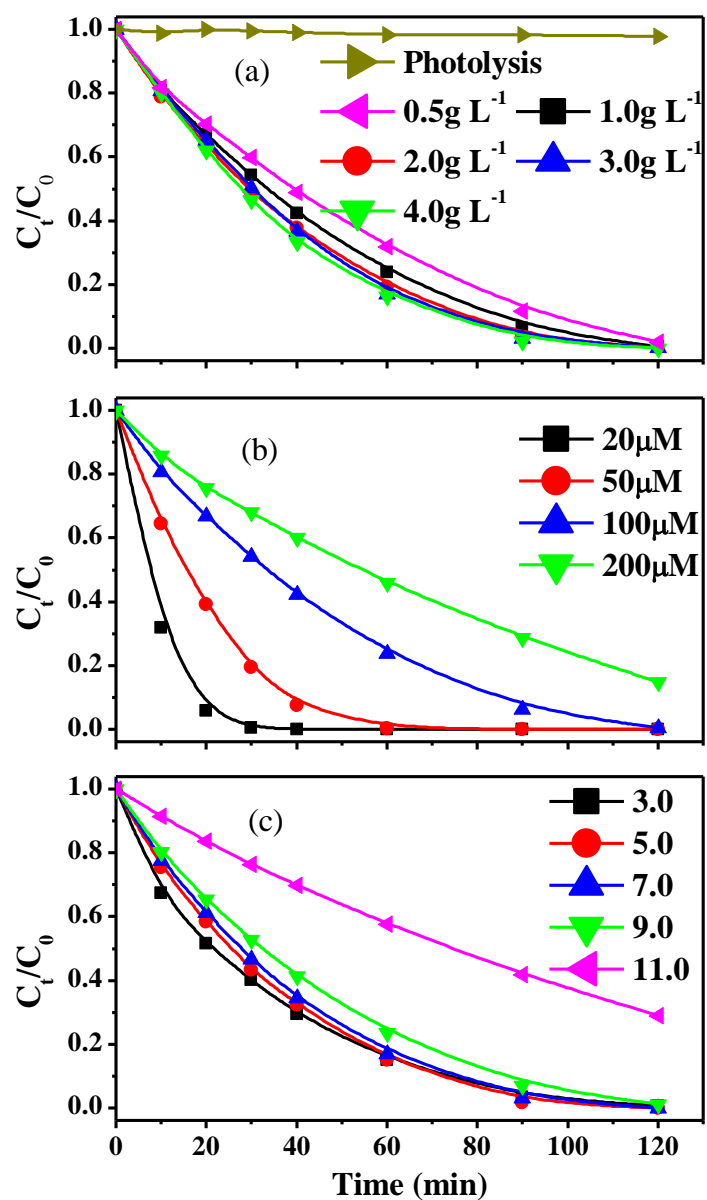
Figure S3 Photolysis and photocatalytic degradation of 100 µM PPB with different TiO$_2$ dosages (a), with different initial PPB concentrations (b), with different pH values (c).
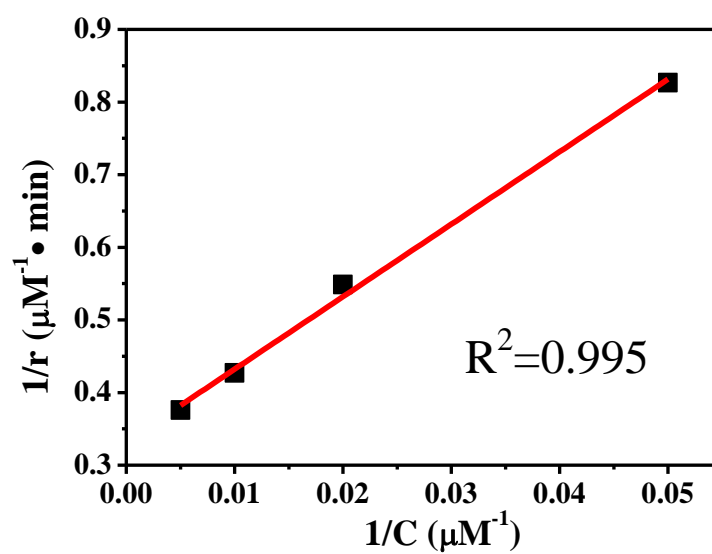
Figure S4 Reciprocal of initial degradation rate (1/r) against the reciprocal of initial concentration of PPB (1/C).
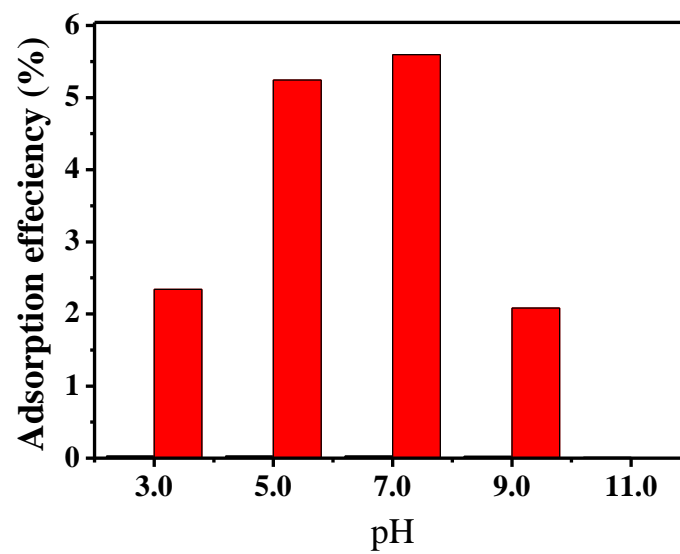
Figure S5 The adsorption efficiencies of PPB onto TiO$_2$ photocatalyst surface stirred in the dark for 30 min at different pH values.
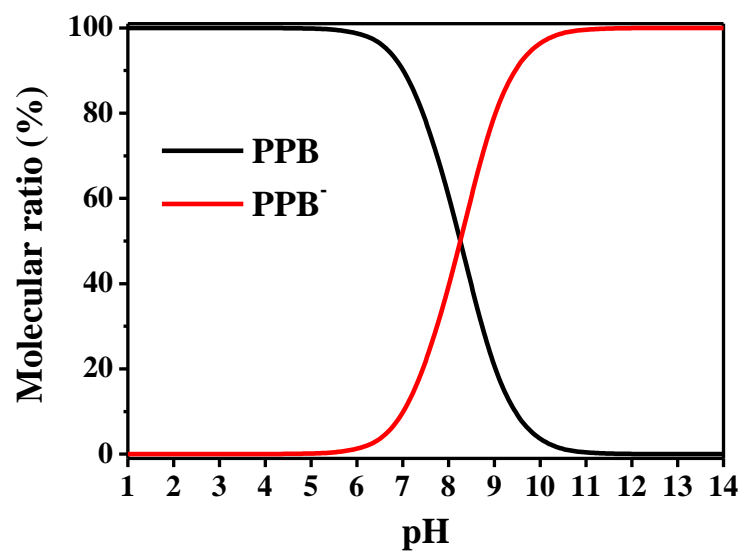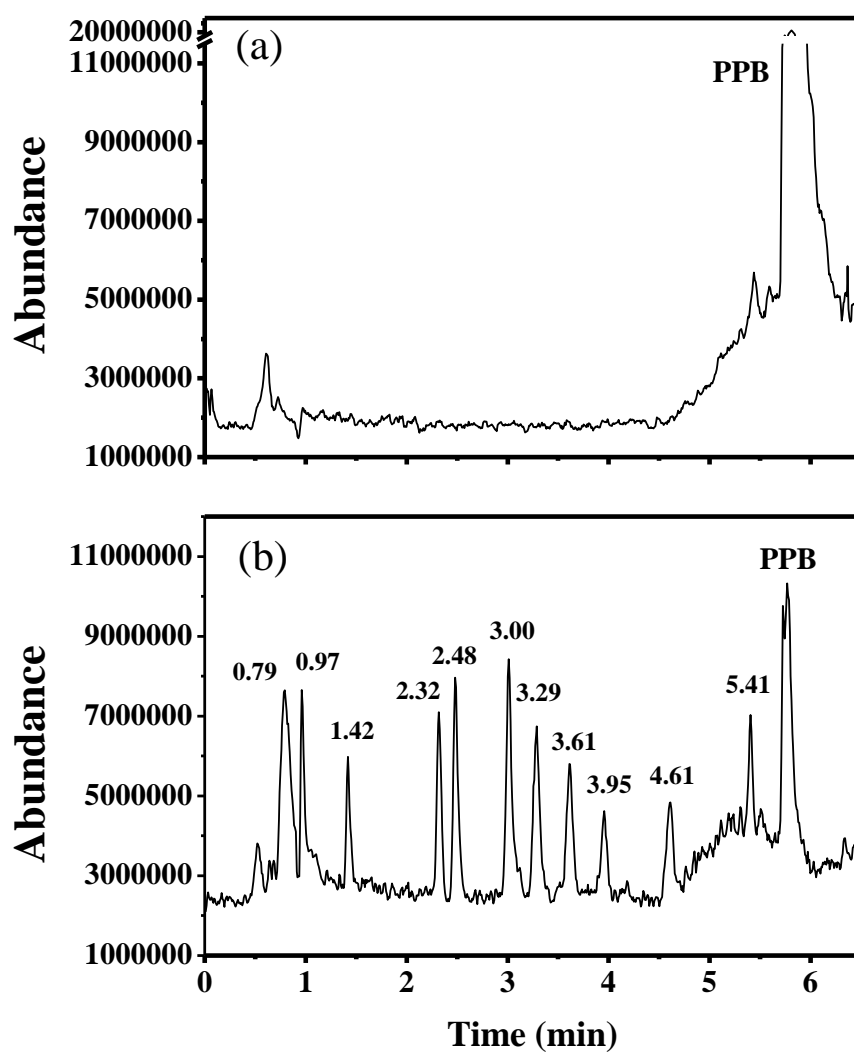
Figure S6 Effect of pH on variation of PPB molecular ratio.

Figure S7 Schematic representation of the photocatalytic processes taking place at a TiO_2 photocatalyst surface under UV irradiation.

Figure S8 TIC chromatogram and the retention times of products obtained by UPLC/MS/MS with ESI‾ mode for (a) 100 μM PPB and (b) photocatalytic degradation sample of 100 μM PPB at 40 min.
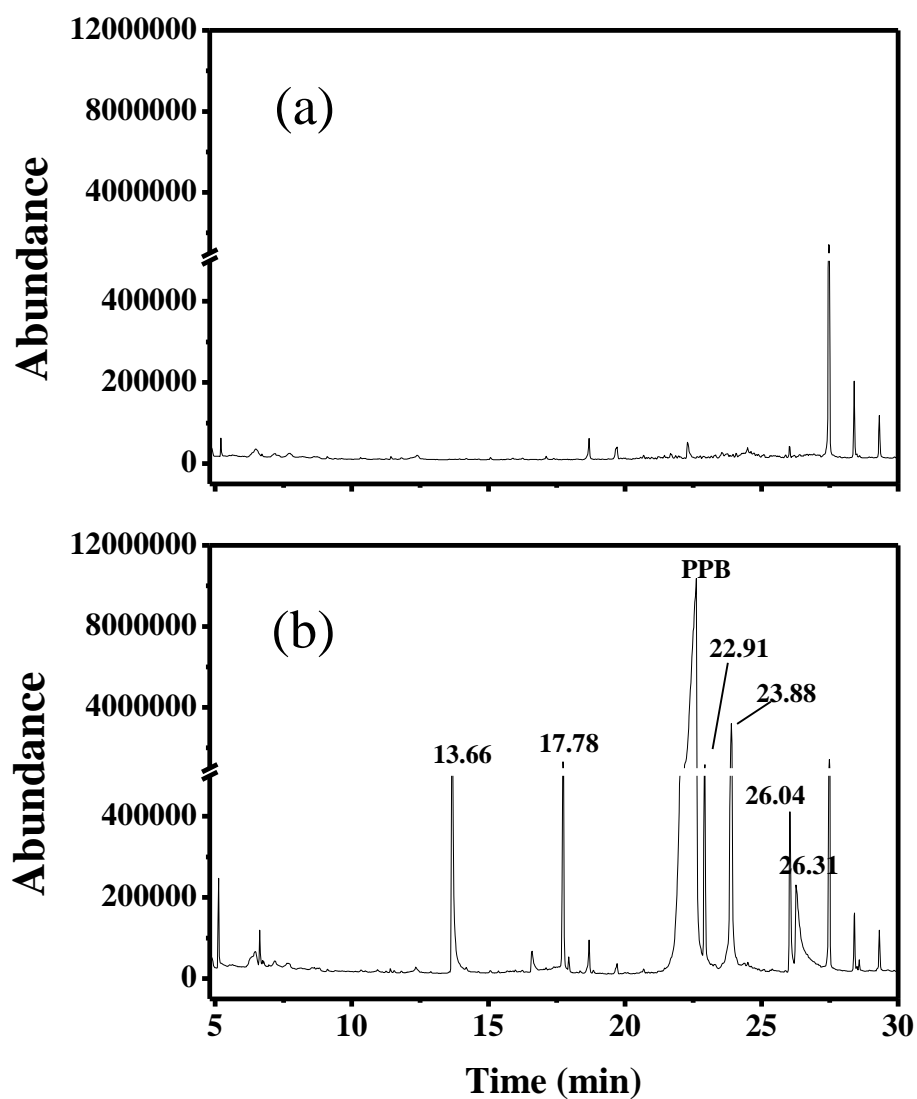
Figure S9 TIC chromatogram and the retention times of products obtained by SPE/GC/MS for (a)

pure water and (b) photocatalytic degradation sample of 100 μM PPB at 40 min.
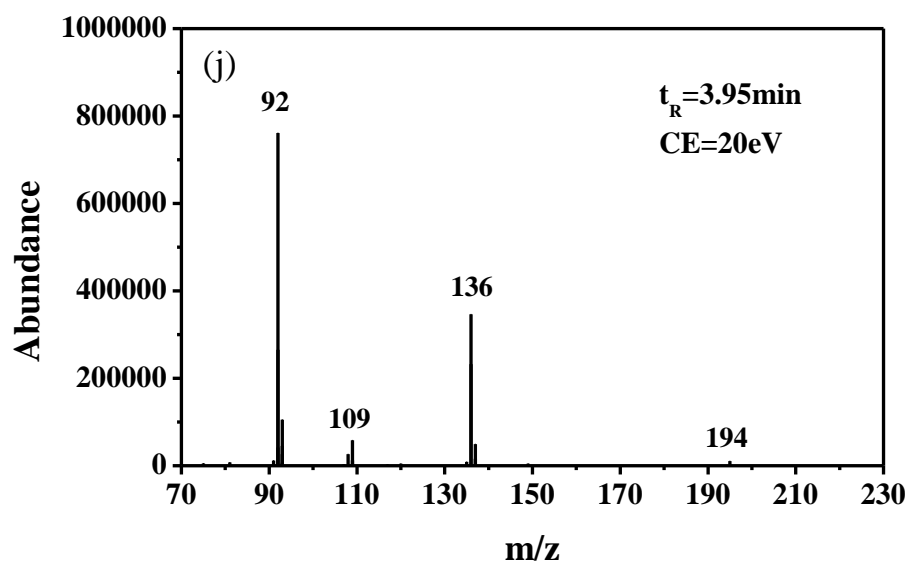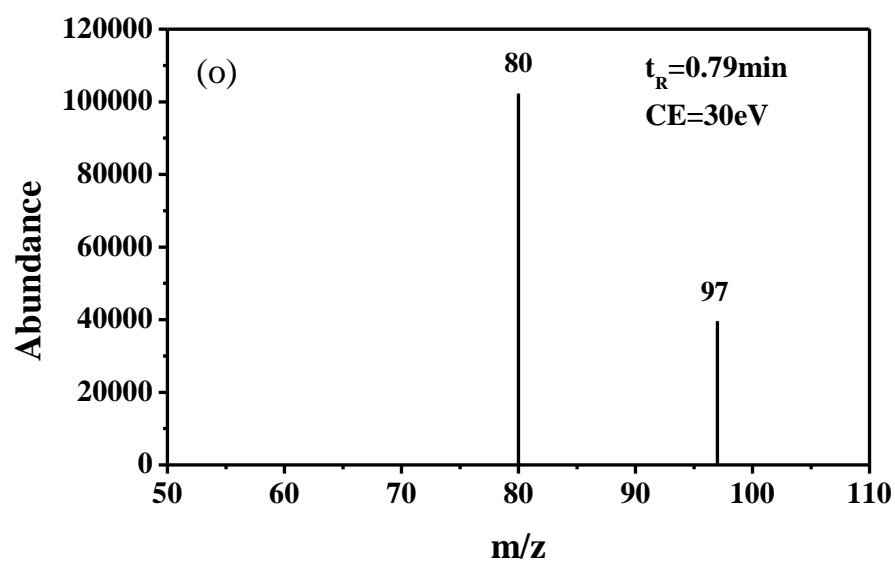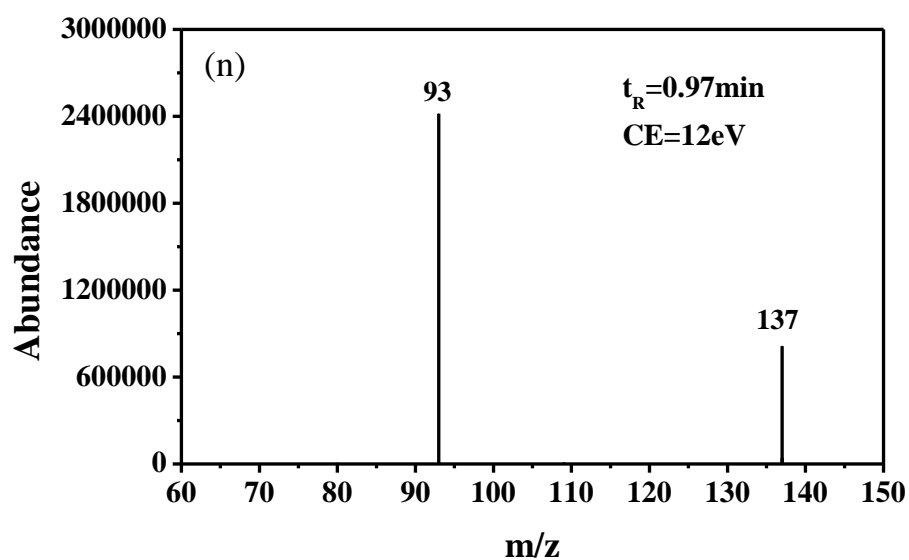
(j) $t_R=3.95min$ CE=20eV

(k) $t_R=4.61min$ CE=10eV

(l) $t_R=4.61min$ CE=20eV
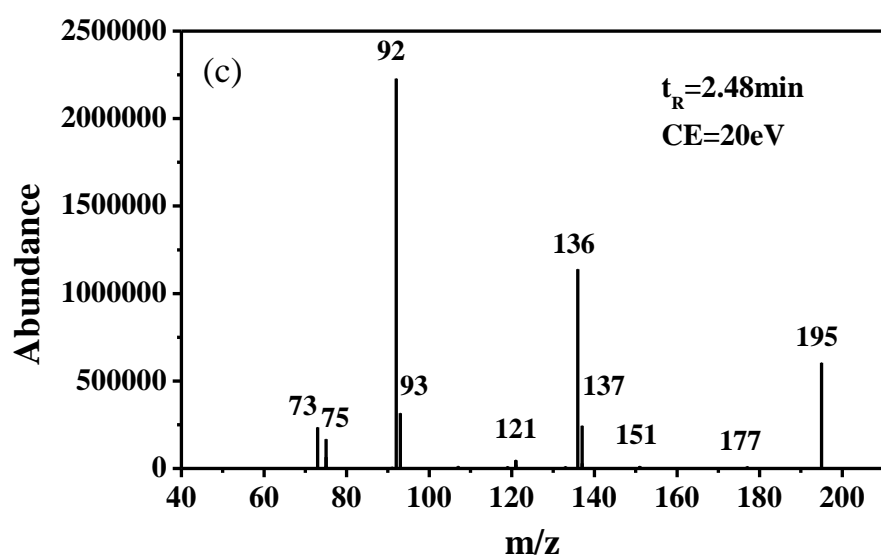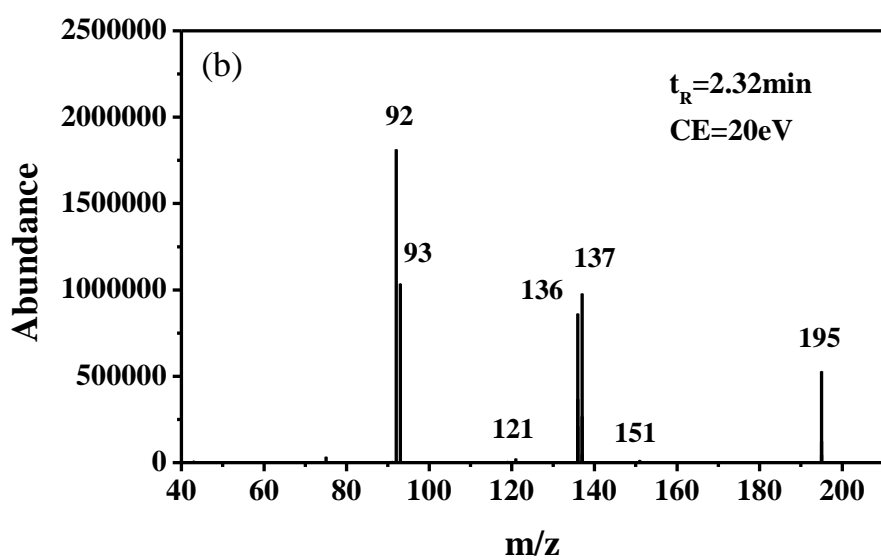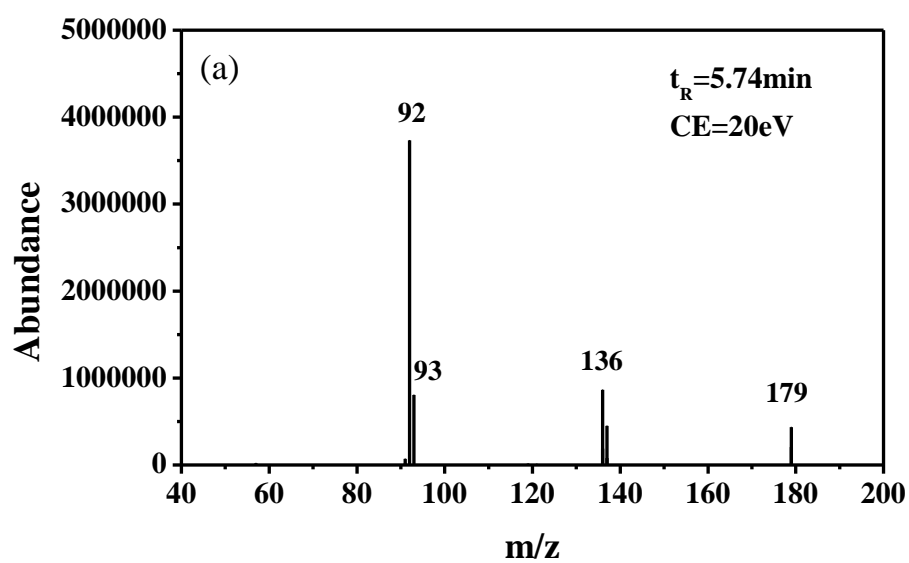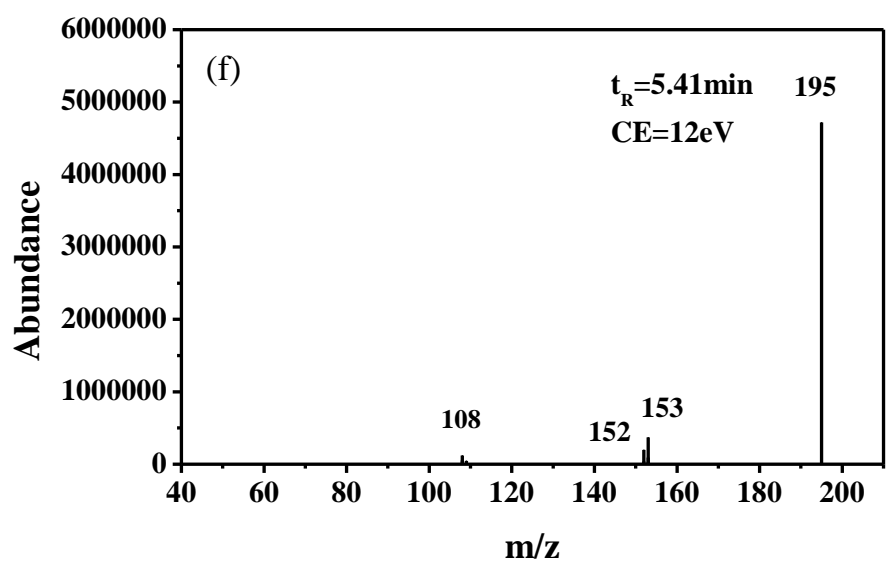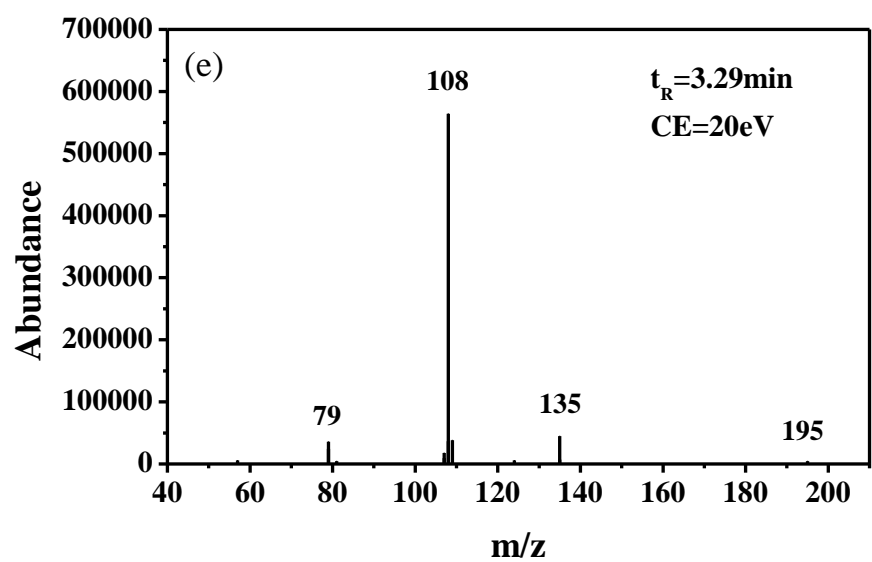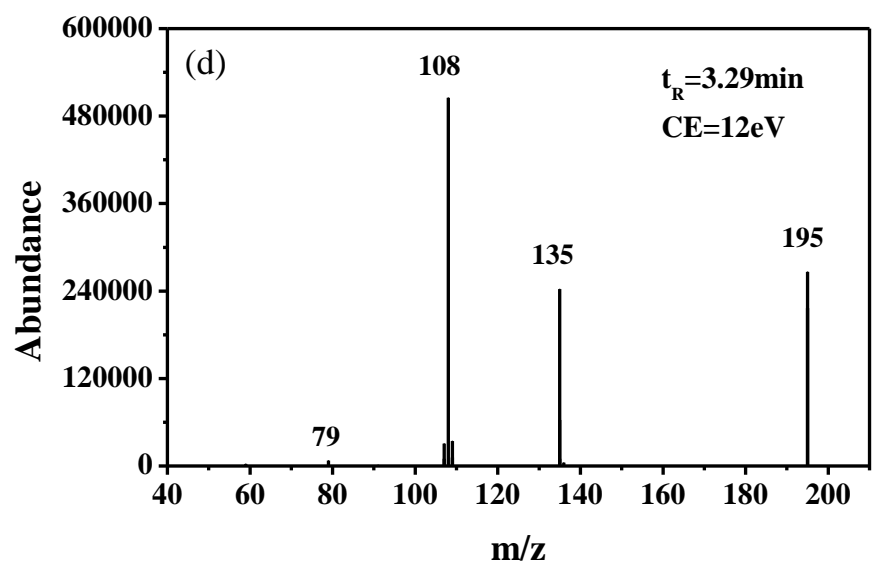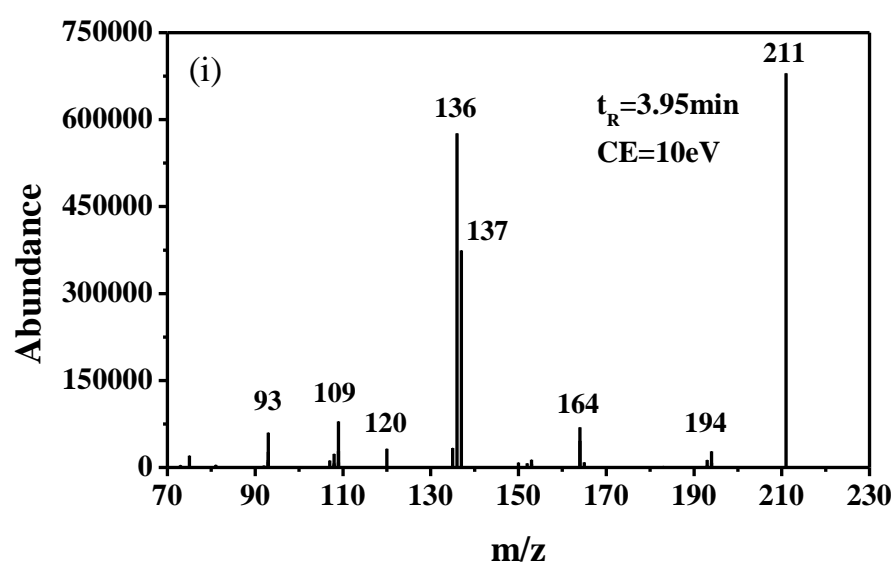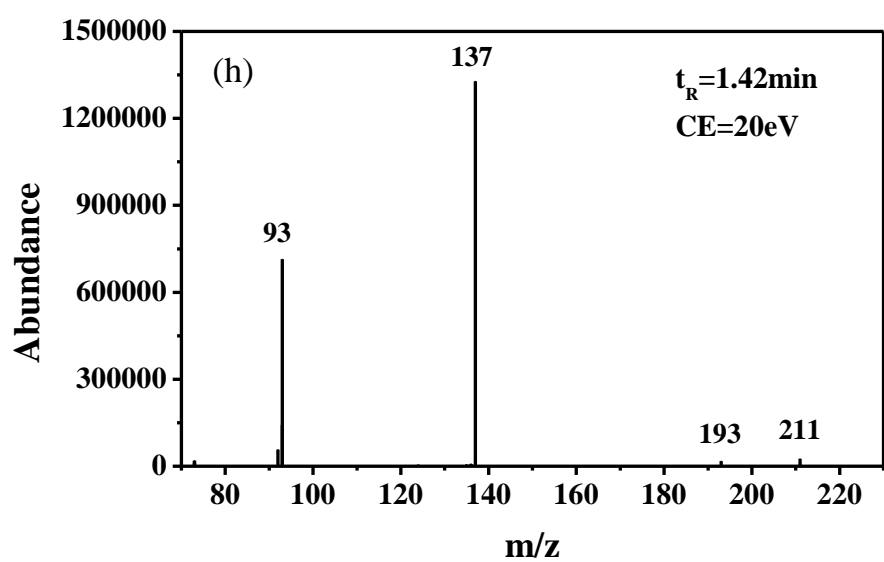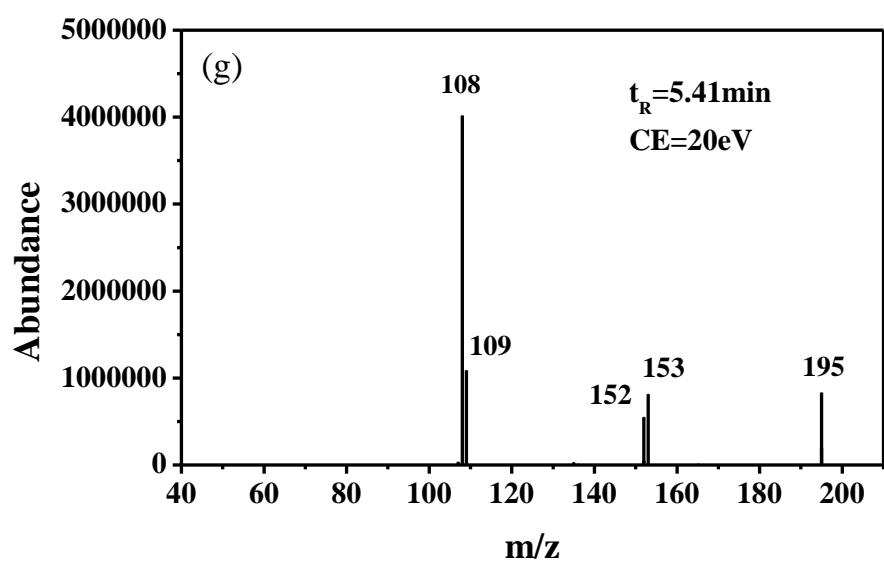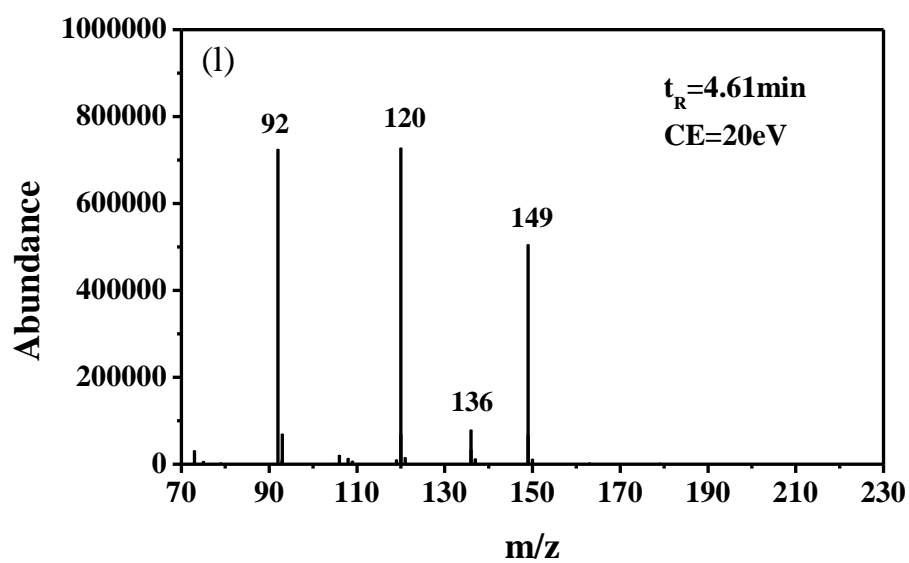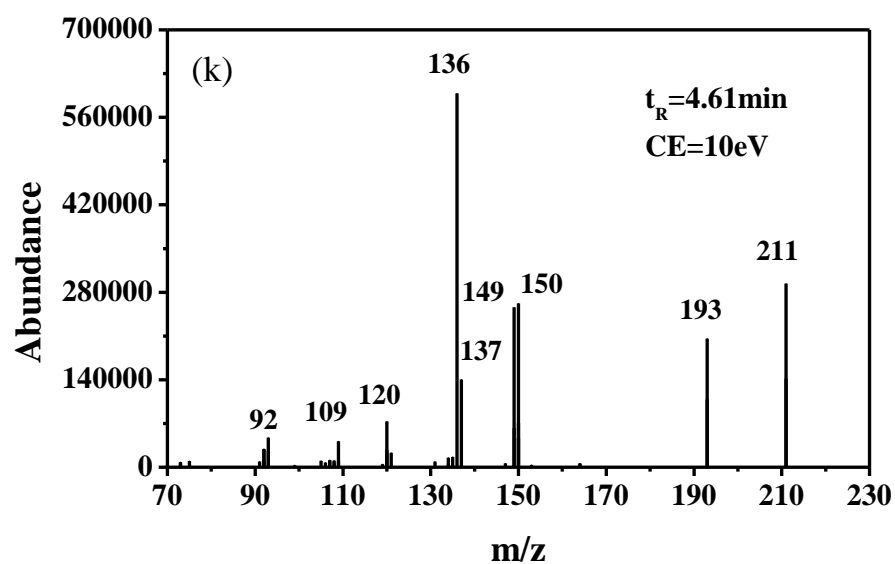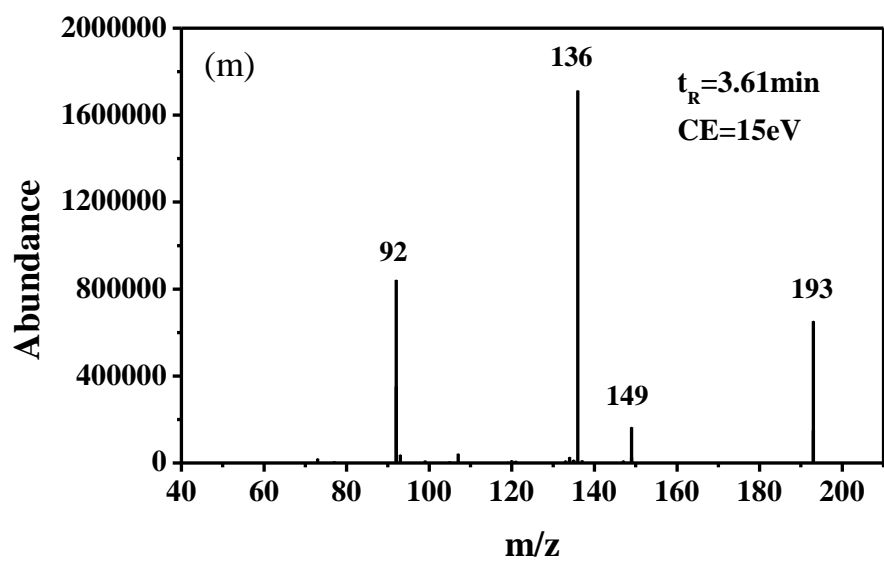
Figure S10 Fragmentation patterns for products identified by UPLC/MS/MS.
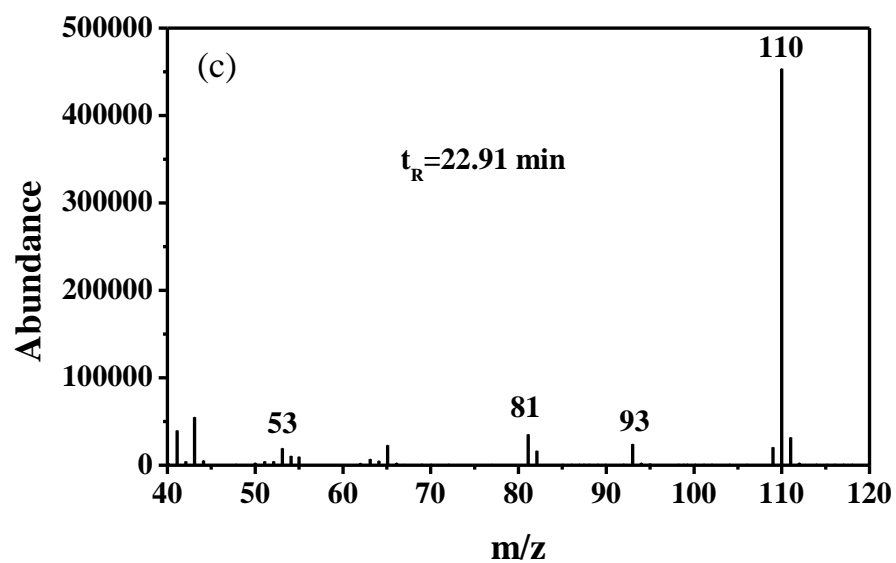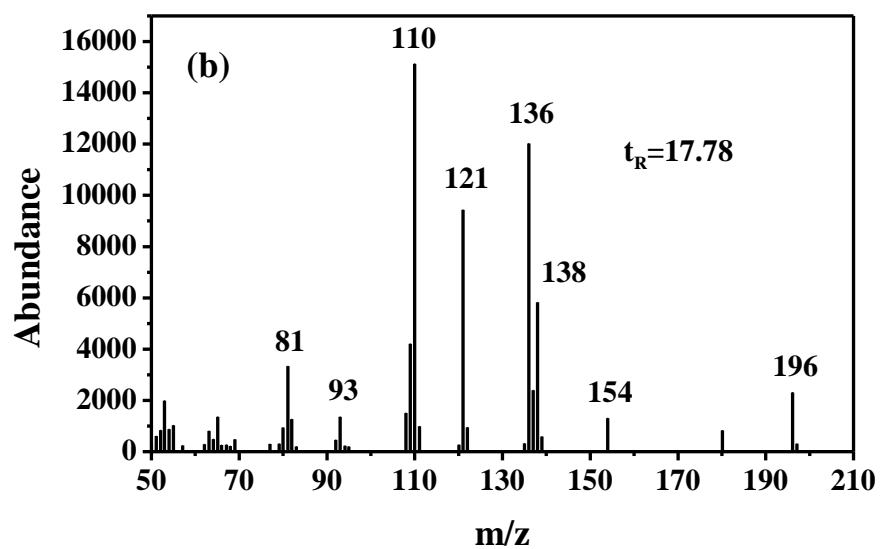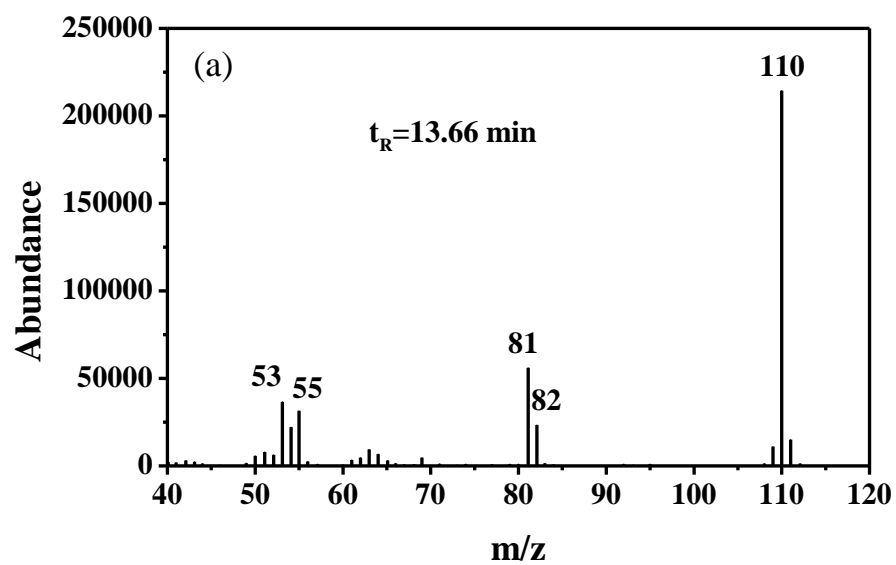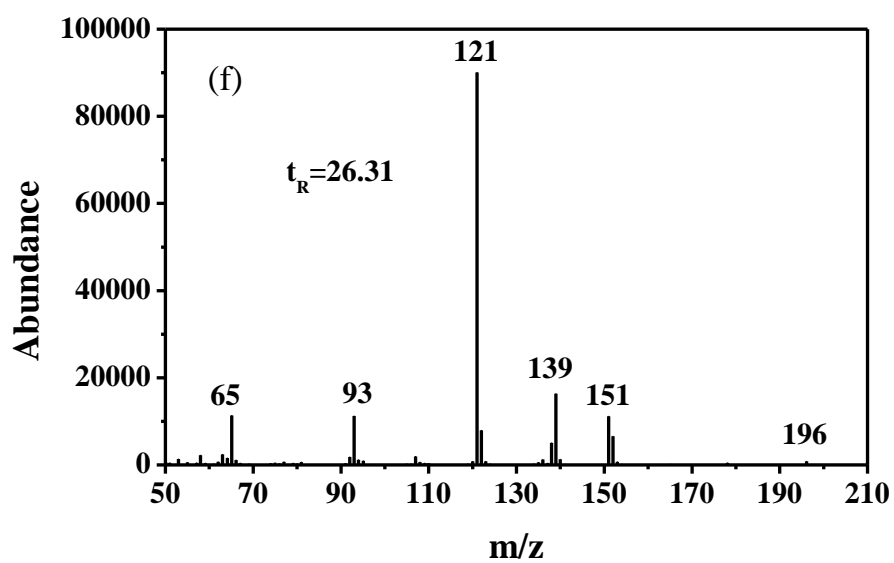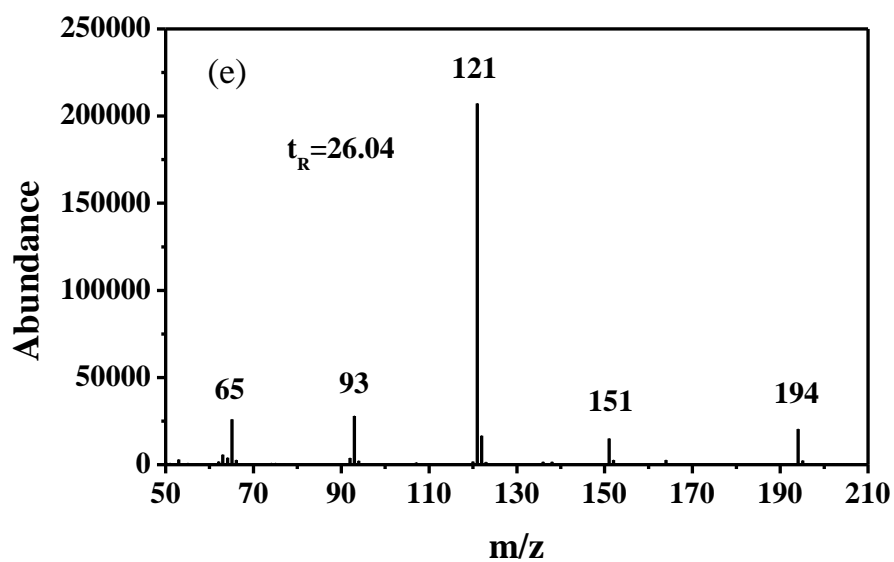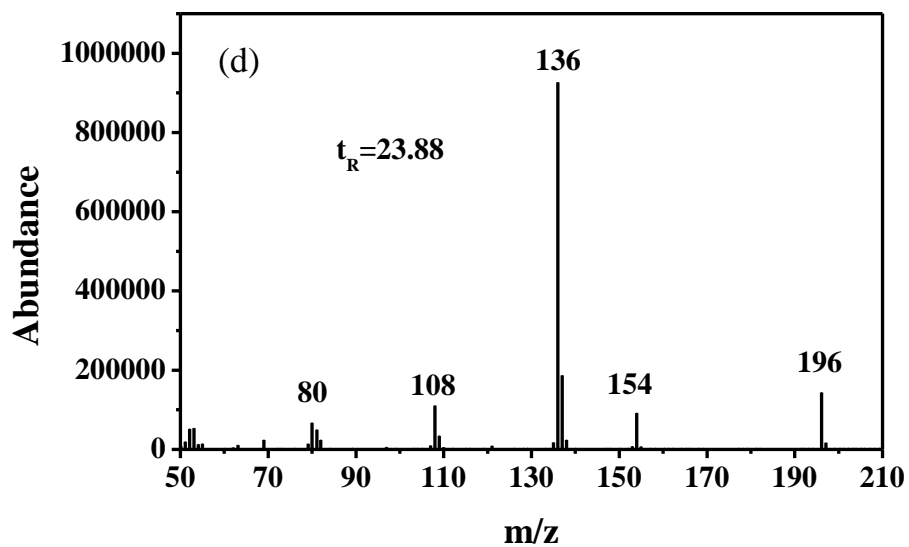
Figure S11 Fragmentation patterns for products identified by SPE/GC/MS.
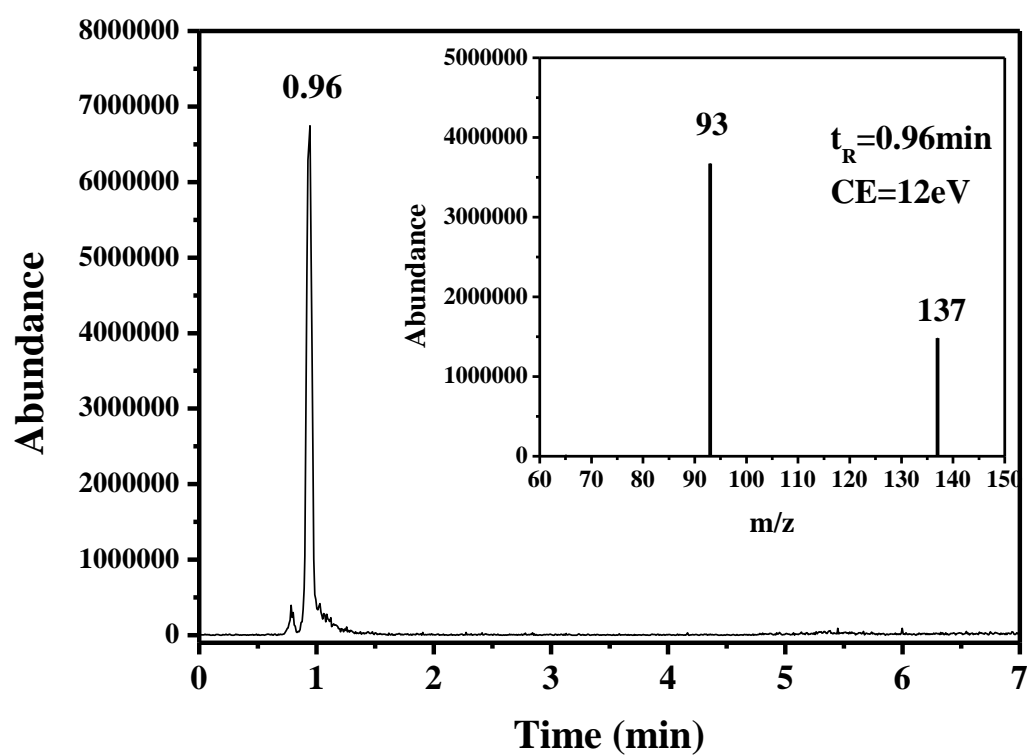
Figure S12 TIC chromatogram and the fragmentation patterns of 20 μM HB obtained by

UPLC/MS/MS with ESI⁻ mode.
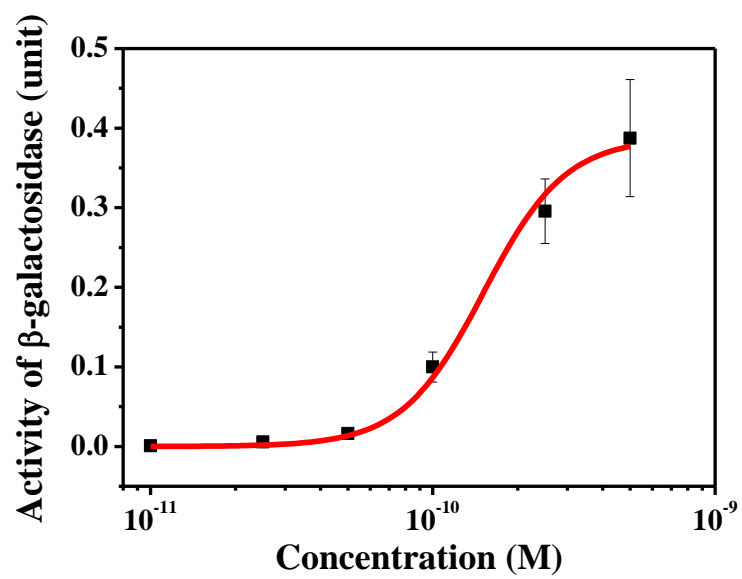
Figure S13 Dose response curve of 17β-estradiol.

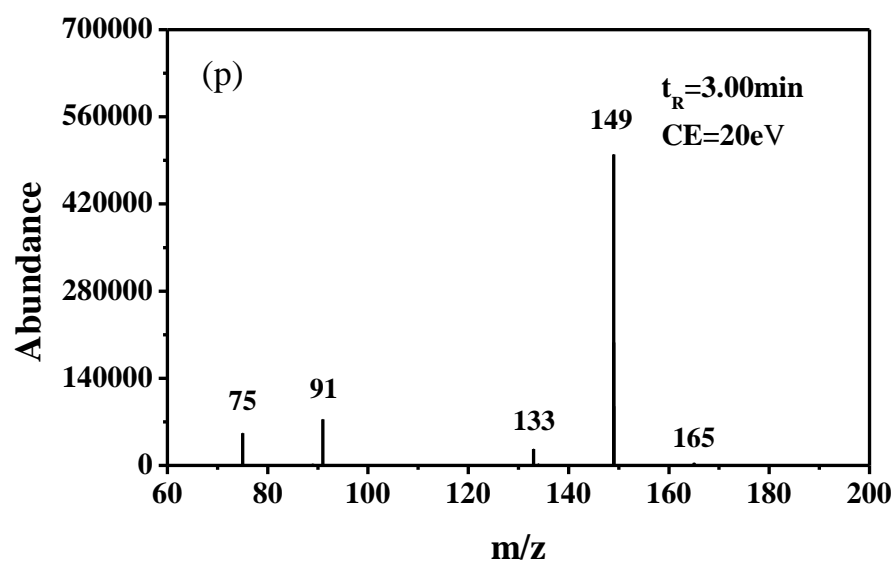(a)

Inset axes: k (μs^{-1}) vs Concentration (μM), $R^2 = 0.998$

0.2 μs 0.5 μs
1.0 μs

ΔA

Wavelength (nm)

(b)

0 μM
50 μM
100 μM
150 μM
200 μM
300 μM
400 μM

Inset axes: A_0/A vs [EPB]/[KSCN], $R^2 = 0.998$

ΔA

Time (μs)
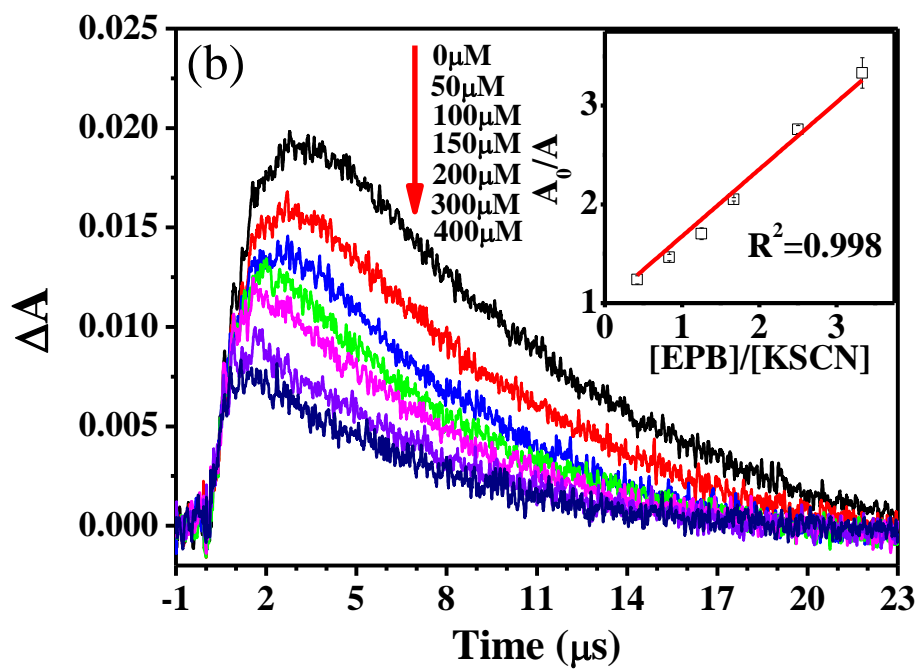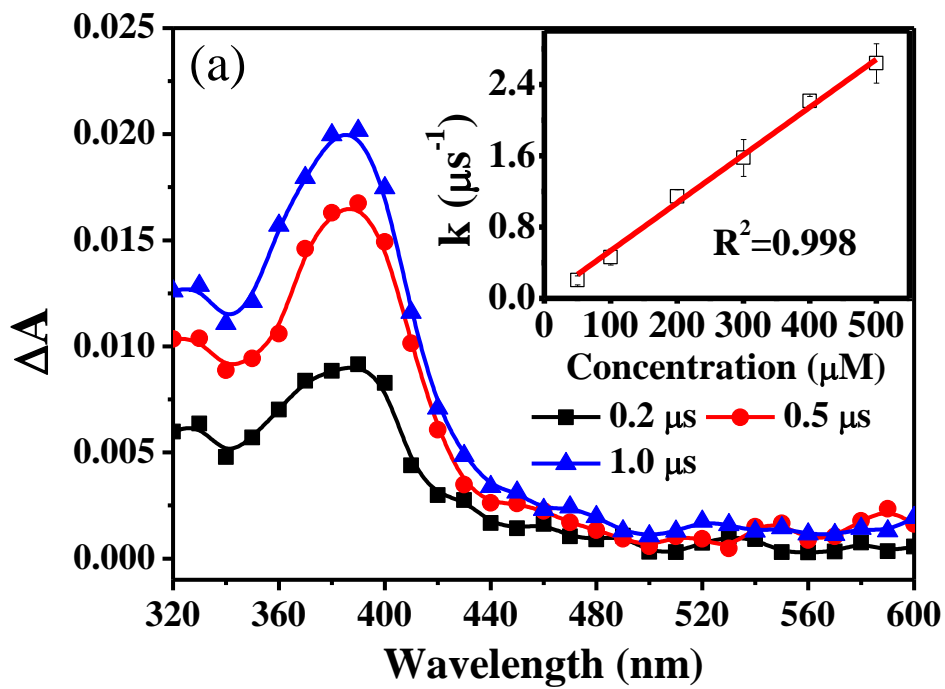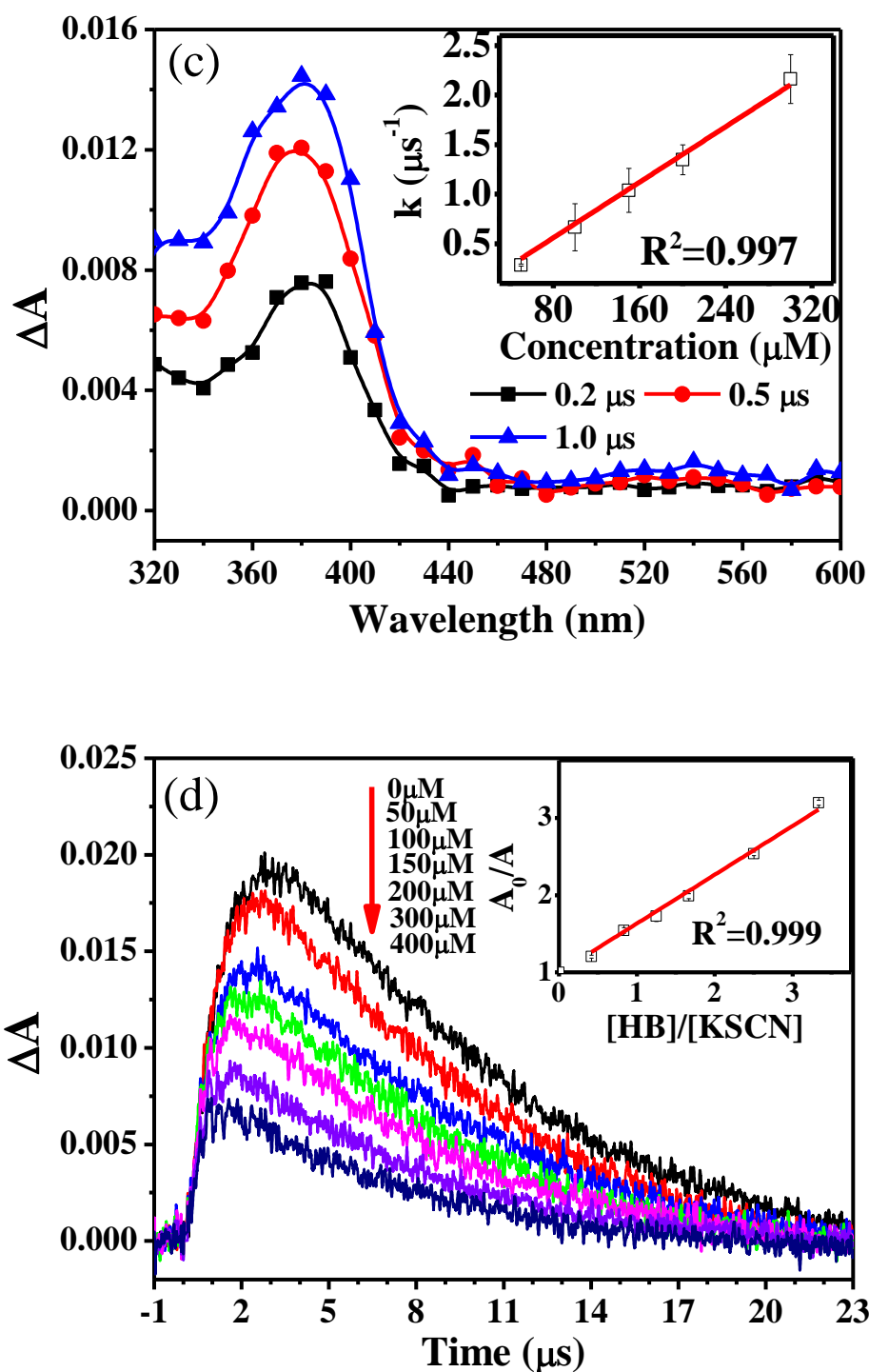
Figure S14 (a) and (c). Difference adsorption spectra of the transient generated from the reaction of 300 μM EPB (a) and 300 μM HB (c) saturated with N_2O. Inset represents the plot of the pseudo-first-order transient formation rate constants at 390 nm (a) or 380 nm (c) vs. different substrate concentrations; (b) and (d). Kinetics observed for N_2O-saturated 120 μM KSCN at 480 nm with different concentrations of EPB (b) and HB (d). Inset represents the competitive plot as a function of the Substrate/KSCN relative concentration.

References

(1) Yang, H.; Li, G. Y.; An, T. C.; Gao, Y. P.; Fu, J. M. Photocatalytic degradation kinetics and mechanism of environmental pharmaceuticals in aqueous suspension of TiO_2: A case of sulfa drugs. *Catal. Today* **2010**, *153* (3-4), 200-207; DOI: 10.1016/j.cattod.2010.02.068.

(2) Lin, Y. X.; Ferronato, C.; Deng, N. S.; Chovelon, J. M. Study of benzylparaben photocatalytic degradation by TiO_2. *Appl. Catal. B-Environ.* **2011**, *104* (3-4), 353-360; DOI 10.1016/j.apcatb.2011.03.006.

(3) Yang, H.; An, T. C.; Li, G. Y.; Song, W. H.; Cooper, W. J.; Luo, H. Y.; Guo, X. D. Photocatalytic degradation kinetics and mechanism of environmental pharmaceuticals in aqueous suspension of TiO_2: A case of beta-blockers. *J. Hazard. Mater.* **2010**, *179* (1-3), 834-839; DOI 10.1016/j.jhazmat.2010.03.079.

(4) Tsai, W. T.; Lee, M. K.; Su, T. Y.; Chang, Y. M. Photodegradation of bisphenol-A in a batch TiO_2 suspension reactor. *J. Hazard. Mater.* **2009**, *168* (1), 269-275; DOI 10.1016/j.jhazmat.2009.02.034.

(5) Zheng, S.; Cai, Y.; O'Shea, K. E. TiO_2 photocatalytic degradation of phenylarsonic acid. *J. Photochem. Photobio. A-Chem* **2010**, *210* (1), 61-68; DOI 10.1016/j.jphotochem.2009.12.004.

(6) Labat, L.; Kummer, E.; Dallet, P.; Dubost, J. P. Comparison of high-performance liquid chromatography and capillary zone electrophoresis for the determination of parabens in a cosmetic product. *J. Pharmaceut. Biomed.* **2000**, *23* (4), 763-769; DOI 10.1016/S0731-7085(00)00358-7.

(7) Teel, A. L.; Warberg, C. R.; Atkinson, D. A.; Watts, R. J. Comparison of mineral and soluble iron Fenton's catalysts for the treatment of trichloroethylene. *Water Res.* **2001**, *35* (4), 977-984; DOI 10.1016/S0043-1354(00)00332-8.

(8) El-Morsi, T. M.; Budakowski, W. R.; Abd-El-Aziz, A. S.; Friesen, K. J. Photocatalytic degradation of 1,10-dichlorodecane in aqueous suspensions of TiO_2: A reaction of adsorbed chlorinated alkane with surface hydroxyl radicals. *Environ. Sci. Technol.* **2000**, *34* (6), 1018-1022; DOI 10.1021/es9907360.

(9) Minero, C.; Mariella, G.; Maurino, V.; Vione, D.; Pelizzetti, E. Photocatalytic transformation of organic compounds in the presence of inorganic ions. 2. Competitive reactions of phenol and alcohols an a titanium dioxide-fluoride system. *Langmuir* **2000**, *16* (23), 8964-8972; DOI 10.1021/la0005863.

(10) Muneer, M.; Bahnemann, D.; Qamar, M.; Tariq, M. A.; Faisal, M. Photocatalysed reaction of few selected organic systems in presence of titanium dioxide. *Appl. Catal. A-Gen.* **2005**, *289* (2), 224-230; DOI 10.1016/j.apcata.2005.05.003.

(11) Giraldo, A. L.; Peñuela, G. A.; Torres-Palma, R. A.; Pino, N. J.; Palominos, R. A.; Mansilla, H. D. Degradation of the antibiotic oxolinic acid by photocatalysis with TiO2 in suspension. *Water Res.* **2010**, *44* (18), 5158-5167; DOI: 10.1016/j.watres.2010.05.011.

(12) Chen, Y. X.; Yang, S. Y.; Wang, K.; Lou, L. P. Role of primary active species and TiO_2 surface characteristic in UV-illuminated photodegradation of Acid Orange 7. *J. Photochem. Photobio. A-Chem* **2005**, *172* (1), 47-54; DOI 10.1016/j.jphotochem.2004.11.006.

(13) Chen, Y. M.; Lu, A. H.; Li, Y.; Zhang, L. S.; Yip, H. Y.; Zhao, H. J.; An, T. C.; Wong, P. K. Naturally occurring sphalerite as a novel cost-effective photocatalyst for bacterial disinfection under visible light. *Environ. Sci. Technol.* **2011**, *45* (13), 5689-5695; DOI 10.1021/es200778p.

(14) Cho, M.; Chung, H.; Choi, W.; Yoon, J. Linear correlation between inactivation of *E. coli* and OH radical concentration in TiO_2 photocatalytic disinfection. *Water Res.* **2004**, *38* (4), 1069-1077; DOI 10.1016/j.watres.2003.10.029.

(15) Zhang, L. S.; Wong, K. H.; Yip, H. Y.; Hu, C.; Yu, J. C.; Chan, C. Y.; Wong, P. K. Effective photocatalytic disinfection of *E. coli* K-12 using AgBr-Ag-Bi_2WO_6 nanojunction system irradiated by visible light: The Role of Diffusing Hydroxyl Radicals. *Environ. Sci. Technol.* **2010**, *44* (4), 1392-1398; DOI 10.1021/es903087w.